Marine Biotechnology (2019) 21:526–536
https://doi.org/10.1007/s10126-019-09900-2

ORIGINAL ARTICLE

RNA Interference by Ingested dsRNA-Expressing Bacteria to Study Shell Biosynthesis and Pigmentation in *Crassostrea gigas*

Dandan Feng[1] · Qi Li[1,2] · Hong Yu[1,2]

Received: 31 January 2019 / Accepted: 16 April 2019 / Published online: 15 May 2019

Abstract

RNA interference (RNAi) is an important molecular tool for analysis of gene function in vivo. Although the Pacific oyster *Crassostrea gigas* is an economically important species with fully sequenced genome, very few mechanistic studies have been carried out due to the lack of molecular techniques to alter gene expression without inducing stress. In this present study, we used unicellular alga *Platymonas subcordiformis* and *Nitzschia closterium f. minutissima* as a vector to feed oysters with *Escherichia coli* strain HT115 engineered to express double-stranded RNAs (dsRNAs) targeting specific genes involved in shell pigmentation. A *C. gigas* strain with black shell was used to target *tyrosinase* or *peroxidase* gene expression by RNAi using the above-mentioned approach. The results showed that feeding oyster with dsRNA of *tyrosinase* could knock down the expression of corresponding *tyrosinase* and hinder the developed shell growth. Feeding oyster with dsRNA of *peroxidase* could knock down the expression of the corresponding *peroxidase* and result in reduced black pigmentation in the newly developed shell. This non-invasive RNAi study demonstrated that *tyrosinase* played a vital role in the assembly and maturation of shell matrices and *peroxidase* was essential for black pigmentation in the shell. Moreover, the RNA interference by ingested dsRNA-expressing bacteria is a relatively simple and effective method for knockdown of a gene expression in adult oysters, thus further advances the use of *C. gigas* as model organism in functional genomic studies.

Keywords RNA interference · *Crassostrea gigas* · Tyrosinase · Peroxidase · Pigmentation · Biomineralization

Introduction

RNA interference (RNAi) technique can induce post-transcriptional gene silencing in intact organisms and has been widely applied to study loss-of-function effects in various organisms, including fungi, plant, insects, and mammals (Ipsaro and Joshua-Tor 2015; Payton et al. 2017). RNAi was initially described in the nematode *Caenorhabditis elegans* demonstrating that introduction of double-stranded RNA (dsRNA) in cells could induce targeted gene-specific inactivation through degradation of the corresponding endogenous mRNA (Fire et al. 1998). RNAi can be delivered in a variety of ways, for example soaking animals in dsRNA or morpholinos, injecting dsRNA or morpholinos, or feeding dsRNA-expressing bacteria (Rivera et al. 2011). Feeding of dsRNA-expressing bacteria is an inexpensive and high-output technique to produce large quantities of dsRNA (Timmons et al. 2001; Tian et al. 2009; Schumpert et al. 2015).

Colorful shells from mollusca have always attracted interest of naturalist and biologist. However, shell formation and pigmentation have not been well studied compared with other classic bone biomineralization and skin pigmentation (Knoll 2003; Slominski et al. 2004; Du et al. 2017; Williams 2017). Molluscan shells are produced by the outer fold of the mantle. Shells are multi-layered structures made up of calcium carbonate crystals together with proteinaceous material and pigments (Arivalagan et al. 2016). Shell growth and pigmentation are under neurosecretory control (Boettiger et al. 2009; Budd

Electronic supplementary material The online version of this article (https://doi.org/10.1007/s10126-019-09900-2) contains supplementary material, which is available to authorized users.

✉ Qi Li
qili66@ouc.edu.cn

[1] Key Laboratory of Mariculture, Ministry of Education, Ocean University of China, Qingdao 266003, China

[2] Laboratory for Marine Fisheries Science and Food Production Processes, Qingdao National Laboratory for Marine Science and Technology, Qingdao 266237, China

et al. 2014). Shells generally grow in a linear fashion by adding new material to the growing edge that is in contact with the mantle tissue (Jabbour-Zahab et al. 1992; Williams 2017). Recently, large amount of transcriptomic, proteomic, and genomic data have been generated in mollusca, particularly in relation to the shell formation and pigmentation (Williams 2017; McDougall and Degnan 2018). These data provide useful resource for molecular and genetic analyses of shell formation and pigmentation.

The Pacific oyster, *Crassostrea gigas*, is a widely distributed and economically important species in the world. It has been gradually developing into a potential model organism for marine Mollusca studies (Yu et al. 2016). Shell color is highly heritable in *C. gigas* (Evans et al. 2009). Since the first quantitative trait locus (QTL) for pigmentation was discovered by Ge et al. (2014), several additional QTLs have been subsequently identified in *C. gigas* (Ge et al. 2015; Song et al. 2018; Wang et al. 2018). However, because of the low density of the current linkage maps and poor genome assembly, it limits the use of linkage analysis and genome mapping to identify genes involved in shell pigmentation (Hedgecock et al. 2015). Alternatively, genome-wide expression profiling comparing selected Pacific oyster lines of different shell colors has identified candidate genes of shell pigmentation (Feng et al. 2015; Feng et al. 2018). Among these candidates, *tyrosinase*, which belongs to the phenoloxidase family, deserves specific attention as it appears to be highly conserved in melanin synthesis pathway (Vavricka et al. 2014). In addition, peroxidase has been suggested to serve in an alternative melanogenic pathway in insect and cephalopod (Palumbo 2003; Christensen et al. 2005). In a previous study, *tyrosinase* LOC_105324831 and *peroxidase* LOC_105324712 have been identified to potentially involve in melanin pigmentation in *C. gigas* shell by RNA-seq (Feng et al. 2018).

In spite of the availability of a fully sequenced genome of *C. gigas*, very little mechanistic studies have been carried out in oysters due to the lack of molecular techniques to manipulate gene expression (Zhang et al. 2012; Schumpert et al. 2015; Li et al. 2018). RNAi has become a powerful tool to alter gene expression. However, the traditional delivery method of injection would produce wound and stress and hamper the growth. Recent studies reported that a feeding-based, non-invasive RNAi approach was effective in triggering a specific RNAi response in *C. gigas* (Payton et al. 2017). This Trojan horse strategy used the dinoflagellate *Heterocapsa triquetra* as a vector for the dsRNA-producing *E. coli* HT115. It combined bacteria–algae interaction with bacterial engineering to generate non-invasive RNAi in filter feeders, which was applied to the study of biological rhythms.

In this study, a feeding-based RNAi experiment was conducted to characterize shell growth and pigmentation in *C. gigas*. Genes encoding *Tyrosinase* and *Peroxidase* enzymes that are potentially critical for melanin synthesis in oyster were selected as the targets for RNAi. We used a *C. gigas* strain with a characteristic whole black shell as our model. Expression of the targeted genes, shell growth, and melanin pigmentation were characterized in the newly developed shell. The data provide evidence for establishment of an easy, feeding-based RNAi method in *C. gigas* to study shell formation and pigmentation.

Materials and Methods

Oyster and Algal Culture

Seven-month-old Pacific oysters with whole black shell (60 individuals; shell length, 47.6 ± 5.4 mm) were collected from culture population in Weihai, Shandong, China (May 2018). Oysters were randomly stuck with labels, divided into 3 groups of 20 oysters, and placed into 3 tanks of 40 l aquarium equipped with an open circulatory system of natural seawater (30 psu) at a flow rate of 12 ml min^{-1}. They were acclimated 10 days before the start of the experiment and continuously fed with *Platymonas subcordiformis* (25,000 cells ml^{-1}) and *Nitzschia closterium f. minutissima* (35,000 cells ml^{-1}) at a flow rate of 12 ml min^{-1}. Alga *P. subcordiformis* and *N. closterium f. minutissima* cultures were grown in f/2 medium using sterilized seawater. Cultures were maintained at 19 ± 1 °C, under a light:dark (L:D) 14:10 cycle. *P. subcordiformis* has four flagellates and is 16–30 μm long; *N. closterium f. minutissima* has no flagellate and is 12–23 μm long.

Vector Construction and Expression of dsRNA

We selected the L4440 vector for generating dsRNAs in an inducible manner in *E. coli.* This vector contains two convergent T7 polymerase promoters in opposite orientation separated by a multi-cloning site (Timmons et al. 2001). The *tyrosinase* transcript (*CgTyr*) and *peroxidase* transcript (*CgPer*) were targeted for degradation by RNAi. DNA fragments of *CgTyr* and *CgPer* were amplified from *C. gigas* by PCR using specific primers (704 bp, from positions 210 to 913 of the 2016-bp-long *tyrosinase* gene, XM_020065712.1, LOC_105324831; 718 bp, from positions 1715 to 2432 of the 3165-bp-long *peroxidase* gene, XM_011423866.2, LOC_105324712; Table 1, Fig. 1). Appropriate restriction enzyme sites were engineered into the 5′ ends of both PCR primers for sub-cloning (Table 1). *Enhanced Green Fluorescent Protein* (*EGFP*) was used as a negative control in the experiments as it did not have a natural target RNA in *C. gigas.* Fragments were purified and ligated into L4440 (Abgene) vectors, which were used to transform DH5α bacteria (Takara, China). Noted for each construct, the bacteria were cultured in Luria Broth (LB) containing 100 μg ml^{-1} ampicillin. L4440 (Abgene), generating constructed vectors

Table 1 A summary of primer sequence used in this study

Primer names	Primer sequences	Experiment
RNAi-Per2-F-SpeI	CTAGACTAGTCCGATTTGGTCACAGTATGAT	Plasmid construction
RNAi-Per2-R-HindIII	CCAAGCTTGTCGTTTTTGAATTCTGA ACAAG	
RNAi-Tyr1-F-HindIII	CCAAGCTTTGGAGTAATCAGTTCTTCGGT	
RNAi-Tyr1-R-SpeI	CTAGACTAGTGCCCTAGCTTGTGAACGG	
CgTyrO-F	CCACTGCTGGACGCAATACCTATC	Quantitative real-time PCR
CgTyrO-R	GCTCTACACGCTGTCTCCAACAAC	
CgTyrI-F	ACACGCTGCTAACGACAGGATTG	
CgTyrI-R	GCAACCGATGAAGAGGAAGACGAT	
CgPerO-F	AGCAATGCCGTCCACCAGAGA	
CgPerO-R	GCCGATCCGTCCAGATAGTGAGT	
CgPerI-F	GCCGCCATTAACATCCAGAGAGG	
CgPerI-R	GGCTCCAGTGGTGAACGTAGTG	
EGFP-F	GTGCTTCAGCCGCTACCC	
EGFP-R	GATGTTGCCGTCCTCCTTG	
Gadph-F	CGTACCAGTTCCAGATGTTTCC	
Gadph-R	GCCTTGATGGCTGCCTTAATA	
EFI-F	CAAGAACGGAGATGCTGGTATGG	
EFI-R	TTTCACTCTTTCCACCGGCTTT	

F and R designate forward and reverse primers, respectively

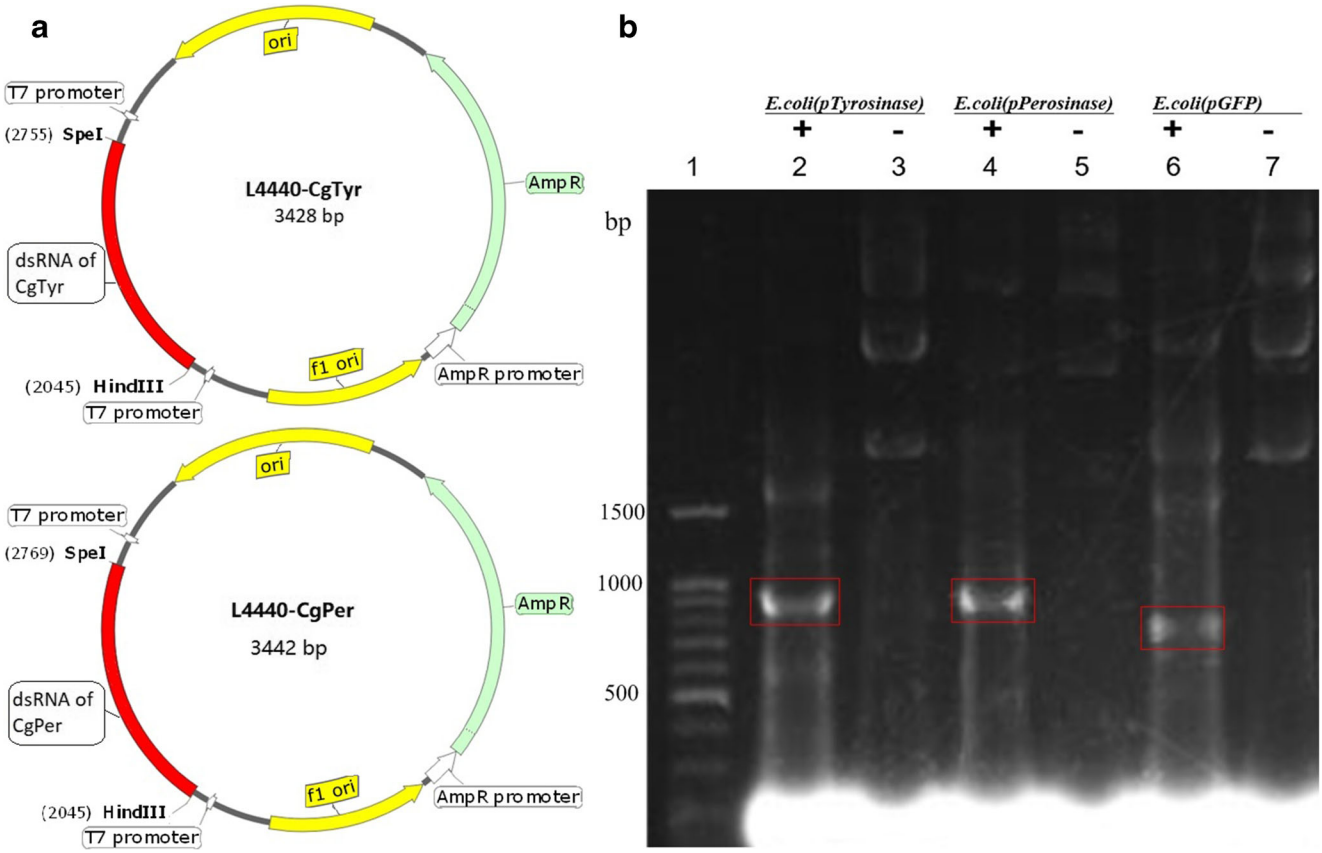

Fig. 1 Plasmid constructs and induction assays. **a** Plasmid construction of *CgTyr*-L4440, *CgPer*-L4440 with *CgTyr*, and *CgPer* fragment sizes and total plasmid sizes. **b** Lane 1 in gel electrophoresis corresponded to a 100 bp DNA ladder (Transgene, China). Red box indicated bands associated with *Tyrosinase* (lane 2) and *Peroxidase* (lane 4) double-stranded RNAs, from RNA extraction of the IPTG-induced *E. coli* transformed with *CgTyr*-L4440 and *CgPer*-L4440

CgTyr-L4440, *CgPer*-L4440, and *EGFP*-L4440, was confirmed by sequencing. Competent *E. coli* cells HT115 (F-, mcrA, mcrB, IN (rrnD-rrnE) 1, lambda-, rnc14::Tn10 (DE3 lysogen: lavUV5 promoter-T7 polymerase)), lacking the dsRNA-specific endonuclease RNase III, were used to produce high level of specific dsRNAs (Timmons et al. 2001). HT115 (DE3) competent cells were prepared using standard $CaCl_2$ methodology and were transformed with *CgTyr*-L4440, *CgPer*-L4440, and *EGFP*-L4440, respectively.

RNAi Feeding Procedures

During the interference phase, three tanks of black shell oysters were continuously exposed to the Alga/dsRNA-producing bacteria co-inoculum. Three dsRNA-producing bacteria were prepared by inducing *E. coli* strain HT115 (DE3) bacteria transformed with three constructed plasmids (*CgTyr*-L4440, *CgPer*-L4440, and *EGFP*-L4440) with isopropylβ-D-thiogalactoside (IPTG). Algae/bacteria co-inoculum was produced by mixing algal culture and bacterial suspension at a ratio of 100 bacteria per algal cell, with a final *P. subcordiformis* concentration of 25,000 cells ml^{-1} and *N. closterium f. minutissima* concentration of 35,000 cells ml^{-1}. The ratio was optimized by increasing algal concentration according to Payton et al. (2017). Food reserves were renewed with fresh algae/bacteria co-inoculum every 24 h. Specifically, *E. coli* strain HT115 bacteria containing recombinant plasmid were grown overnight with shaking in LB with ampicillin (50 μg ml^{-1}) and tetracycline (12.5 μg ml^{-1}) at 37 °C. Five milliliter of overnight culture was diluted 100-fold in 500 ml of fresh LB medium containing ampicillin (50 μg ml^{-1}) and tetracycline (12.5 μg ml^{-1}) and allowed to grow to $OD_{595} = 0.4$. dsRNA production was induced by 0.4 mM IPTG for 4 h at 37 °C under agitation. Then, induced bacterial cultures were centrifuged and bacterial pellets were re-suspended in 500 ml *P. subcordiformis* and 125 ml *N. closterium f. minutissima* algae culture liquid. The bacteria could be either attached to the algae or free-living (Doucette 1995). Bacteria adsorption rate on the algae was evaluated by preliminary experiments. Briefly, algae/bacteria inoculum was filtrated through 5 μm pore size (Xinya, Shanghai, China) and was spread on LB agar (100 μg ml^{-1} ampicillin), as well as the total inoculum. The adsorption rate was assessed as the ratio between the number of colonies from filtrated suspension and from total inoculum, which was calculated as 99%. Concentrations of algae and bacteria were monitored daily with SP-721 UV–visible spectrophotometer (Shanghai, China) for the duration of the experiment.

Mantle tissues from 10 oysters per condition were individually sampled at the end of the interference phase (day 15 and day 35). There is no oyster dying during the 15- and 35-day exposure experiments. A total of 60 oysters were dissected. All research experiments were performed in accordance with our institutional guidelines.

Phenotypic Change Statistical Analyses

Computer vision (CV) is a technology that includes image capturing, processing, and analyzing. CV enables an objective and nondestructive assessment of color patterns in non-uniformly colored surfaces and determining other physical features, such as image texture, morphological elements, and defects (Timmermans 1998; Pedreschi et al. 2006). *L*a*b** is an international standard for color measurements, adopted by the Commission International d' Eclairage (CIE) in 1976 (Timmermans 1998). *L** is the luminance or lightness component, which ranges from 0 to 100, and parameters *a** (from green to red) and *b** (from blue to yellow) are two chromatic components, which range from − 120 to 120 (Papadakis 2000). We photographed shells of oysters according to Evans et al. using a digital camera (Nikon D4) (Evans et al. 2009). Individual oyster from the three groups was classified either having the obviously newly developed shell or not, comparing with photo at the start of the RNAi experiment. The newly developed shell pigmentation was recorded based on five categories with five index numbers (Takeo and Sakai 1961). The categories were described as follows:

0- Whole surface is gray white with no black coloration
1- A small part of newly developed shell is black colored
2- Nearly half part of newly developed shell is black colored
3- Most part of newly developed shell is black colored
4- All part of newly developed shell is black colored

The percentages of oyster individuals with newly developed shell and the color parameters of the *L**(lightness), *a**-(redness), and *b**(yellowness) of the newly developed shells were analyzed (Hunter 1975; Chakraborty et al. 2014). The lightness, a, and b values obtained in Photoshop CS6 (Adobe System Incorporated, USA) were not standard color values and should be converted to *L*a*b** values using the following formulas (Yam and Papadakis 2004):

$$L^* = \frac{\text{Lightness}}{255} \times 100$$

$$a^* = \frac{240\text{a}}{255} - 120$$

$$b^* = \frac{240\text{b}}{255} - 120$$

Differences between variables (the color parameter) were investigated using a two-tailed Student's *t* test assuming equal variance or chi-square analysis. For all statistical results, a probability of $p < 0.05$ was considered significant. Analyses were performed with IBM SPSS Statistics 20.0 (SPSS, USA).

Total RNA Extraction and qPCR Analyses

RNA extraction was performed on individual sample using TRIzol reagent (Ambion, USA), following the manufacturer's instruction. The total RNA of 1 μg was subjected to reverse transcription using PrimeScript™ RT reagent kit with gDNA Eraser (TaKaRa, China). Relative quantification of gene expression was estimated for each gene using the $^{\triangle\triangle}$Ct method (Schmittgen and Livak 2008). Primer sets were designed from full cDNA sequences of *CgPer*, *CgTyr*, *EGFP*, *glyceraldehyde 3-phosphate dehydrogenase* (*Gadph*) (Payton et al. 2017), and *elongation factor I* (*Ef1*) (Renault et al. 2011) which were used as reference genes (Table 1). All primers were searched using BLASTn in NCBI to ensure matching the specific sequence. The primer sets (*CgPerO*) for qPCR analysis of endogenous *Peroxidase* mRNA levels were derived from the region outside the cloned fragment of *CgPer* to avoid amplification of RNAi products (*CgPer* dsRNA). The primer sets (*CgPerI*) were designed in the region inside the cloned fragment. Similarly, the primer sets *CgTyrO* and *CgTyrI* were designed outside and inside of the cloned fragment of *CgTyr*, respectively. The qPCR was carried in triplicate for each sample on a LightCycler 480 real-time PCR instrument (Roche Diagnostics, Burgess Hill, UK) using SYBR1 Premix Ex TaqTM (TaKaRa, China). Cycling parameters were 95 °C for 5 min and then 40 cycles at 95 °C for 5 s and 60 °C for 20 s. Melting curve analyses were performed following the PCR to verify specific amplification. PCR efficiency (E) was assessed for each primer pair by determining the slope of standard curves obtained from cDNA serial dilution analyses of different experimental samples. Relative gene expression data was analyzed using the comparative threshold cycle (Ct) $2^{-\triangle Ct}$ method, where $\triangle Ct = Ct\ (\text{interest gene}) - Ct\ (\text{housekeeping gene})$. Interest gene values were normalized in each sample with *Ef1* housekeeping gene level, as no significant differences in Ct values were observed in *Ef1* among conditions. Results were expressed as number of copies of gene per copy of *Ef1*.

Data were examined for homogeneity of variances (F text) and were analyzed by *t* test using software SPSS 20.0 with $p < 0.05$. The detection of RNAi products (interest gene dsRNA) in oyster mantles was assessed as the mean ± SE of individuals $2^{-(\triangle Ct(CgInside) - \triangle Ct(CgOutside))}$, i.e., the ratio of the *CgTyr* mRNA level measured with primer sets *CgTyrI* (quantification of both endogenously expressed *CgTyr* mRNAs and *CgTyr* dsRNAs) to the *CgTyr* mRNA level obtained with primer sets *CgTyrO* (quantify the endogenously expressed *CgTyr* mRNAs). Therefore, this ratio is equal to (*gene* dsRNAs + *gene* mRNAs) / *gene* mRNAs = (*gene* dsRNAs / *gene* mRNAs) + 1.

Result

Plasmid Constructs and Induction Assays

The expression of dsRNAs was induced in respective engineered *E. coli* strain with 0.4 mM IPTG for 4 h at 37 °C. Total RNA was isolated from the induced and non-induced bacteria and analyzed via 1% agarose gel electrophoresis. A band of dsRNA corresponding to the *Tyrosinase* gene (704 bp) plus sequence between two T7 promoters of about 200 bp was observed in the IPTG-induced *E. coli* transformed with *CgTyr* construct (Fig. 1, lane 2), but not in the non-induced *E. coli* transformed with *CgTyr* construct (Fig. 1, lane 3), indicating the successful expression of *Tyrosinase* dsRNA in *E. coli*. Similarly, a band of dsRNA corresponding to the *Peroxidase* gene (716 bp) plus flanking about 200 bp sequence was observed in the IPTG-inducing *E. coli* transformed with the *CgPer* construct (Fig. 1, lane 4), but not in the non-induced *E. coli* transformed with the Cg*Per* construct (Fig. 1, lane 5), indicating the successful expression of *Peroxidase* dsRNA in *E. coli*.

Impact of RNAi on Phenotypic Change

Oysters were fed with alga mixed with three different types of *E. coli* culture expressing distinct types of dsRNAs. No effect on animal survival was noted by the RNAi feeding regimen. Shell growth was analyzed in these oysters, and each oyster was classified as having obviously newly developed shell or not (Table 2 and Fig. 2). As shown in Table 2, none of the oysters fed on bacteria-expressing *CgTyr* dsRNA displayed shell growth (Supplementary Fig. S1 and Fig. S2). In contrast, the newly developed shell growth was detected in seven and five oysters from the *Peroxidase* and *EGFP* group, respectively.

As shown in Fig. 2, the newly developed shells showed less and more black pigmentation in the *Peroxidase* or *EGFP* group, respectively. The percentage of black pigmentation area and the *L*a*b** value of the newly developed shell were calculated to show the variations in melanin loss phenotype (Table 2, Fig. 3). Oysters showing greater than 50% loss of black pigmentation in the newly developed shell were classified as loss of melanin, compared with the images at the start of the experiment. It is noteworthy that the area of newly developed shell showing red was classified as loss of black pigment area. Majority of oysters (four out of seven) in the *Peroxidase* group that showed the loss of melanin had a partially clear shell with black pigmentation in only 50% or less shell area. As is shown in Table 2, all oysters (five out of five) fed on *E. coli*-expressing dsRNA *EGFP* showed a no significant change in shell black pigmentation. In contrast, a larger number of oysters in the *Peroxidase* group displayed the black pigmentation loss phenotype, which was four times greater

Table 2 Phenotypic change of *C. gigas* characterized by whole black shell after dsRNA interference

Group		No. 0	No. 1	No. 2	No. 3	No. 4	No. 5	No. 6	No. 7	No. 8	No. 9	Growth shell (%)	Pigmentation loss (%)
Tyrosinase	Day 15	0	0	0	0	0	0	0	0	0	0	0.0	–
	Day 35	0	0	0	0	0	0	0	0	0	0		
Peroxidase	Day 15	0	0	1/2	1/3	0	1/2	0	1/4	1/2	0	35.0	57.1
	Day 35	0	1/2	0	1/3	0	0	0	0	0	0		
EGFP	Day 15	0	0	0	1/4	0	0	1/4	0	0	1/3	30.0	0.0
	Day 35	1/3	0	0	0	0	0	0	1/4	0	0		

Individual was denoted as 0 or 1 corresponding to showing obviously newly secondary shell or not; newly secondary shell pigmentation was recorded as five categories with five index numbers

than the non-target controls. As shown in Fig. 2, oysters fed on bacteria-expressing *CgPer* dsRNA (No. 35 and No. 41) displayed a remarkable loss of black pigmentation. Oysters in the group fed on the *CgTyr* dsRNA-producing bacteria neither showed visible shell growth nor represented loss of black pigmentation. Oysters with obvious shell growth showed significant difference in L^* between the *Peroxidase* and *EGFP* groups (75.92 ± 2.6 and 63.33 ± 7.8, respectively, $p < 0.05$) (Fig. 3). The loss of black pigmentation was evident in the *Peroxidase* group compared to the *Tyrosinase* group.

Detection of RNAi Product in Mantle Tissues

To determine the effectiveness of dsRNA delivery to oyster mantle tissues by feeding, we analyzed *EGFP* dsRNA in oysters fed on bacteria containing the *EGFP*-L4440 plasmid. EGFP dsRNA expression was detected in oysters fed on bacteria containing the *EGFP*-L4440 plasmid but not in oysters fed on *CgPer*-L4440 or *CgTyr*-L4440 (Fig. S3). The detection of RNAi products (*CgTyr* or *CgPer* dsRNA) in oyster mantles was assessed as a function of the ratio of the interfering *CgTyr*/*CgPer* dsRNAs to endogenous *CgTyr*/*CgPer* mRNA level (Fig. S3). Significant amount of RNAi products was found in *CgTyr* dsRNA oysters compared to *EGFP* dsRNA oysters at day 15 ($p = 4.9 \times 10^{-7}$) and at day 35 ($p = 9.2 \times 10^{-6}$). Significant amount of RNAi products was also found in *CgPer* dsRNA oysters at day 15 ($p = 4.1 \times 10^{-4}$). This is consistent with the dsRNA entrance in mantle tissues during the phase of interference treatment. At day 15, the levels of dsRNAs were 2.3 and 2.0 times more abundant than endogenously expressed mRNAs in the *CgTyr* dsRNA and

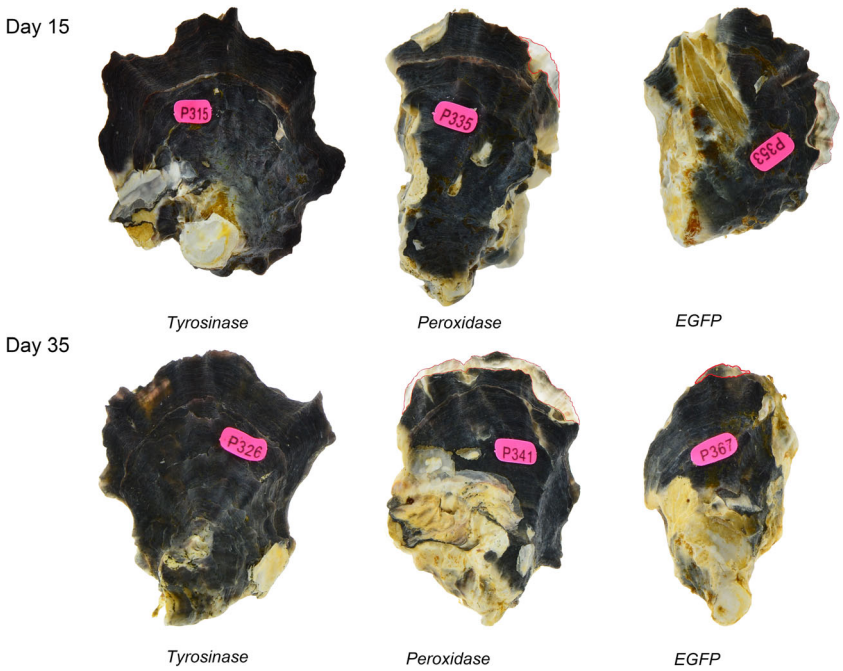

Fig. 2 Analysis of shell growth and pigmentation in newly developed shell. Photographic representation of *C. gigas* from groups *Tyrosinase*, *Peroxidase*, and *EGFP*, which are also classified by day 15 and day 35

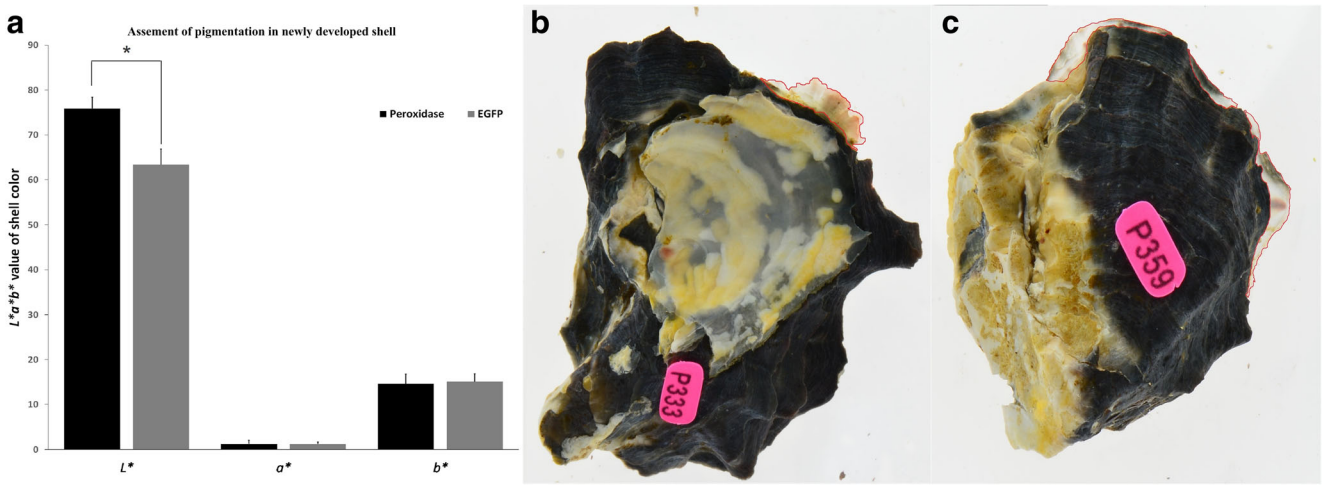

Fig. 3 The analysis of *L*a*b** value of newly developed shell. **a** Comparison of *L*a*b** value of newly developed shell between group *Peroxidase* and group *EGFP*. **b** Photographic representation of *C. gigas* from group *Peroxidase*. **c** Photographic representation of *C. gigas* from group *EGFP*

CgPer dsRNA oysters, respectively. At day 35, the levels of dsRNAs were 1.5 and 2.6 times more abundant than endogenously expressed mRNAs in RNAi-treated oysters expressing the *CgTyr* dsRNA and *CgPer* dsRNA, respectively.

Efficiency of RNAi on the Target Gene Transcription

Since there was a phenotypic change in *C. gigas* fed on bacteria-expressing *CgTyr* or *CgPer* dsRNA, we analyzed the corresponding mRNA levels by qPCR. qPCR results showed that oysters fed on bacteria containing *CgTyr*/*CgPer*-L4440 dsRNA constructs showed reduced *CgTyr*/*CgPer* expression compared to control-treated tissues. As shown in Fig. 4, *CgTyr* or *CgPer* mRNA levels were markedly diminished in *C. gigas* fed on bacteria-expressing *CgTyr* or *CgPer* dsRNA as compared to controls at day 15. In the *Tyrosinase* group, these results were significant and the relative *CgTyr* mRNA expression levels dropped down to ~21% of the control values. Thus, average knockdown was ~79%, with a maximum knockdown value of ~94% ($p = 0.048$) at day 15 (Fig. 4). A significant decrease (57%) was observed in *CgPer* transcripts in the oysters in the *Peroxidase* group at day 15 compared to the *EGFP* dsRNA oysters ($p = 0.036$). There was no significant difference in *CgTyr* transcripts between the *Tyrosinase* group and the control ($p = 0.669$) at the end of interference exposure (day 35, Fig. 4) nor in *CgTyr* ($p = 0.284$) at the end of the experiment (day 35). It is noteworthy that the *CgTyr* and *CgPer* mRNA levels showed diminished tendency at day 35, with decrease of 18 and 33% in the corresponding group. At day 15, individual analysis revealed that 80% of individuals in the *Tyrosinase* group and 30% of individuals in the *Peroxidase* group showed decreased gene expression by more than 70% compared to the control (Fig. 5). At day 35, 30% of individuals in the *Tyrosinase* group and 30% of individuals in the *Peroxidase* group showed decreased gene expression by more than 70% compared to the control (Fig. 5).

Discussion

We explored the potential use of dsRNA via feeding in uncovering gene function involved in biomineralization and pigmentation in *C. gigas*. It has been reported in mollusca that shell color is regulated by shell matrix proteins (SMPs) expressed in different shell layers. While some of these proteins may have a role in shell color determination, it is also possible that these genes may play other roles in shell construction (Berland et al. 2011). It has been suggested that *tyrosinase* plays various roles involving biomineralization, melanogenesis, and innate immunity (Feng et al. 2017). *Peroxidase* has also been identified in the biomineralization toolkit of *Pinctada margaritifera* and *C. gigas*, suggesting a role in the quinone-tanning of shell protein-like *tyrosinase* (Zhang et al. 2012; Arivalagan et al. 2017). The biochemical pathways in the melanogenesis in *Sepia* involve *tyrosinase*, *dopachrome-rearranging enzymes*, and *peroxidase* (Palumbo 2003; Derby 2014), which suggested that *tyrosinase* and *peroxidase* play important roles in melanogenesis of mollusca. A total of 26 *tyrosinase* genes were identified from *C. gigas* genome, of which 13 genes were highly expressed in mantle (Zhang et al. 2012). *Peroxidase* genes have also gone through an expansion and accumulated up to 26 genes, of which nine were highly expressed in the mantle (Feng et al. 2017). Our previous studies reported that the *tyrosinase* (LOC105324831) and *peroxidase* (LOC105324712) are highly expressed in the mantle and they exhibit different patterns

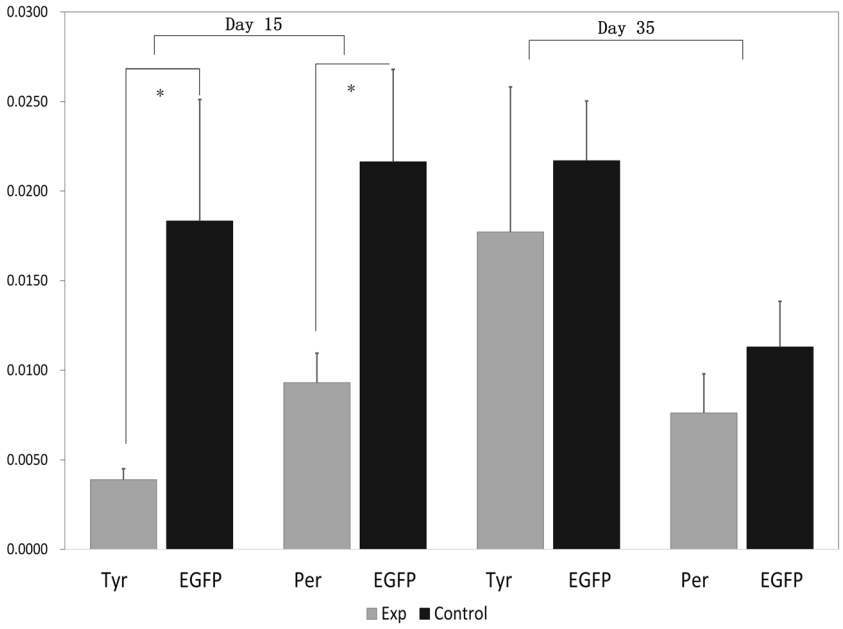

Fig. 4 Quantitation of gene expression levels after RNAi treatment in *Crassostrea gigas*. Levels of respective gene transcripts relative to EfI transcripts analyzed by qPCR and expressed as number of copies of interest gene per copy of EfI in the mantle of oysters at the end of interference day 15 and day 35 phases, expressed in fold change

of expression among *C. gigas* of different shell colors (Feng et al. 2018). Our functional study was designed to validate their roles in biomineralization or pigmentation.

According to previous studies on *C. gigas* (Fabioux et al. 2009; Huvet et al. 2015; Payton et al. 2017), sponges *Tethya wilhelma* and *Ephydatia muelleri* (Rivera et al. 2011),

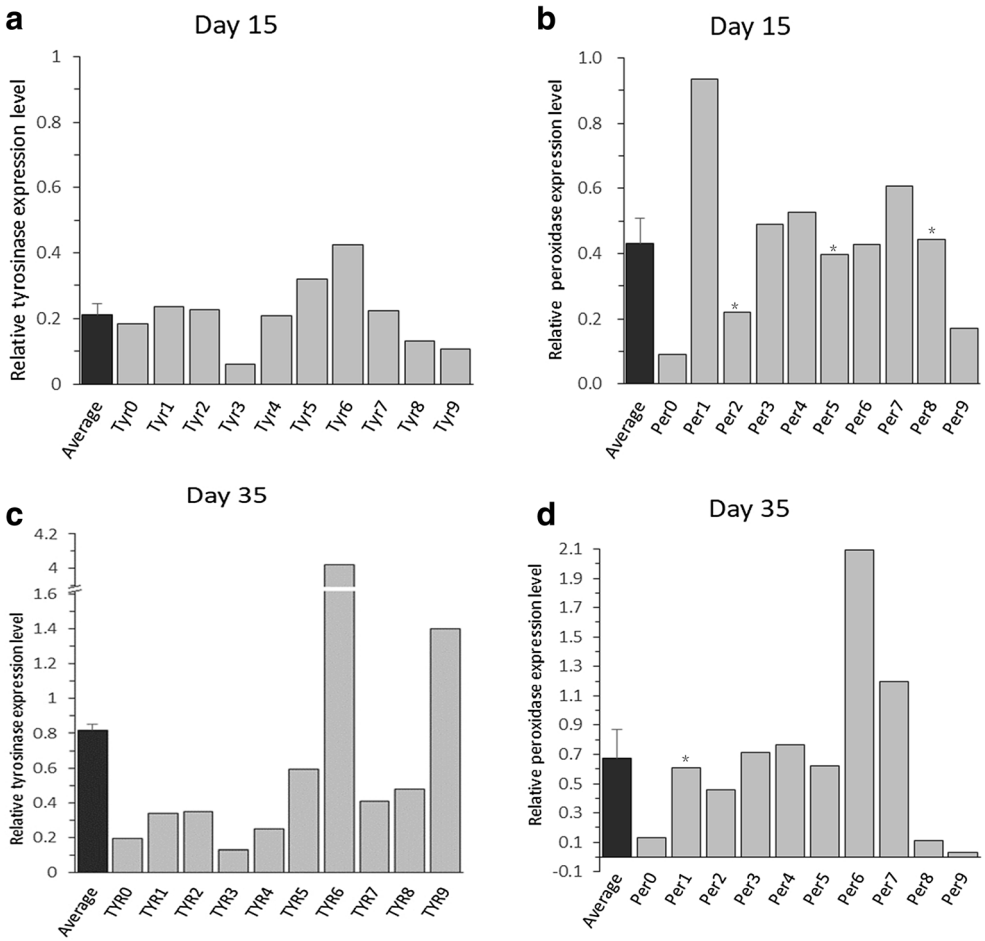

Fig. 5 qPCR assay for gene expression levels of *Tyrosinase* and *Peroxidase* transcript in individual oyster. Expression levels were normalized to FfI and gene expression levels are given as relative levels of RNAi-treated oysters against control oysters. Bars represent standard deviation. Asterisks (*) indicate oysters showing the knockdown phenotype

microcrustacean *Daphnia* (Schumpert et al. 2015), and shrimp *Penaeus monodon* (Sarathi et al. 2008), the maximum effect of dsRNA interference was usually achieved 15 days to 1 month post-induction of dsRNA in *C. gigas* (Fabioux et al. 2009). In this experiment, we performed the knockdown experiment for the period of 35 days in order to obtain a maximum RNAi effect and RNAi phenotype (Payton et al. 2017; Teng et al. 2018). Our data showed that the knockdown of the *Tyrosinase* (XM_020065712.1) or *Peroxidase* (XM_011423866.2) had different effect on shell growth and pigmentation. When the sampled oysters were dissected, we observed many layers of thin transparent shells along the inner shell in the group *Tyrosinase*. None out of 20, seven out of 20, and five out of 20 oyster grew visible new shell edge, respectively from the *Tyrosinase*, *Peroxinase*, and the control group. Accordingly, we proposed that the *CgTyr* could play a vital role in shell biomineralization. This is consistent with previous report that tyrosinase might play a role in biomineralization (Zhang et al. 2012; Du et al. 2017). It has been proposed that dopaquinone production catalyzed by tyrosinase may be essential for the assembly and maturation of both nacreous and prismatic shell matrices.

In order to further compare the melanin levels in the newly developed shell, we compare the color parameters of the *L**(lightness), *a**(redness), and *b**(yellowness) between the *Peroxidase* and the control group. Our data revealed that *C. gigas* with obvious shell growth in the *Peroxidase* group has significantly smaller *L** compared to the *EGFP* group, which means that it is whiter. The *Peroxidase* group also displayed a marked pigmentation loss that was 4 times greater than the non-target controls. Through the RNAi bacterial feeding regimen, the *Peroxidase* group showed the reduction in melanin level. A significant 57% decrease in the mean level of *CgPer* transcripts was observed in oysters at day 15 in the *CgPer* dsRNA condition compared to the control group, suggesting a strong correlation between the loss of melanin and decreased *CgPer* transcription. It has also been proved that *Peroxidase* is associated with melanosomes in the ink gland, where it is thought to catalyze the formation of eumelanin (Gesualdo et al. 1997). It should be noted that all newly developed shell have more or less melanin loss, which can be explained as natural variation or stress response. *C. gigas* can show reduced melanin synthesis if they become stressed. It is possible that the presence of dsRNA could trigger stress response signaling and elicit downstream regulation of melanin production (Schumpert et al. 2015). High variability in RNAi response was observed between individuals, especially for the individuals at day 35. Variation in the amount of dsRNA actually entering into the mantle cells probably contributed to, a large extent, to the variability in RNAi response (Huvet et al. 2015; Fabioux et al. 2009). It should be noticed that *CgTyr* mRNA expression had higher expression level at day 35 than at day 15. When analyzing individual's expression, several individuals at day 35 showed obviously high expression, such as Num. 6 and Num. 9 in the *Tyrosinase* group, which influenced the whole expression change tendency. It has been inferred that a long-term bacteria feeding might influence individual's health and gene normal expression.

It is clear that several parameters need to be optimized to consistently achieve significant knockdown. These include algae/bacteria co-inoculum concentration, the treatment duration, and sample number (Payton et al. 2017). Moreover, the age of oysters also has an effect. Given that none of the sampled oysters died, the amount of bacteria fed to oysters could be further increased for further optimization. It is conceivable that after long period of feeding dsRNA, *C. gigas* might display a macroscopic phenotype that could be detected at the cellular levels, thus additional phenotypical characterization could be included at the cellular and morphological levels.

In conclusion, we showed in this study that the non-invasive RNAi approach through feeding unicellular alga *P. subcordiformis* and *N. closterium f. minutissima* as the vector for the dsRNA-producing *E. coli* HT115 is an efficient method to trigger a specific RNAi response in *C. gigas*. We demonstrated that *tyrosinase* played a vital role in the assembly and maturation of shell matrices and the *peroxidase* was essential for the melanogenesis and pigmentation in the shell.

Acknowledgments This study was supported by grants from the National Natural Science Foundation of China (31772843), the Fundamental Research Funds for the Central Universities (201762014), the Shandong Province (2017LZGC009), and the Taishan Scholars Seed Project of Shandong.

Authors' Contribution D.D.F. performed the experiment, analyzed the data, and wrote the paper. Q.L. and H.Y. conceived and designed the study.

Compliance with Ethical Standards

Competing Interests The authors declare that there is no conflict of interest.

References

Arivalagan J, Marie B, Sleight VA, Clark MS, Berland S, Marie A (2016) Shell matrix proteins of the clam, *Mya truncata*: roles beyond shell formation through proteomic study. Mar Genom 27:69–74

Arivalagan J, Yarra T, Marie B, Sleight VA, Duvernois-Berthet E, Clark MS, Marie A, Berland S (2017) Insights from the shell proteome: biomineralization to adaptation. Mol Biol Evol 34:66–77

Berland S, Marie A, Duplat D, Milet C, Sire JY, Bédouet L (2011) Coupling proteomics and transcriptomics for the identification of novel and variant forms of mollusk shell proteins: a study with *P. margaritifera*. Chembiochem 12:950–961

Boettiger A, Ermentrout B, Oster G (2009) The neural origins of shell structure and pattern in aquatic mollusks. Proc Natl Acad Sci U S A 106:6837–6842

Budd A, McDougall C, Green K, Degnan BM (2014) Control of shell pigmentation by secretory tubules in the abalone mantle. Front Zool 11:62

Chakraborty SK, Singh DS, Kumbhar BK (2014) Influence of extrusion conditions on the colour of millet-legume extrudates using digital imagery. Irish J Agric Food Res 53:65–74

Christensen BM, Li J, Chen C-C, Nappi AJ (2005) Melanization immune responses in mosquito vectors. Trends Parasitol 21:192–199

Derby CD (2014) Cephalopod ink: production, chemistry, functions and applications. Mar Drugs 12:2700–2730

Doucette GJ (1995) Interactions between bacteria and harmful algae: a review. Nat Toxins 3:65–74

Du X, Fan G, Jiao Y et al (2017) The pearl oyster *Pinctada fucata martensii* genome and multi-omic analyses provide insights into biomineralization. GigaScience 6:gix059

Evans S, Camara MD, Langdon CJ (2009) Heritability of shell pigmentation in the Pacific oyster, *Crassostrea gigas*. Aquaculture 286: 211–216

Fabioux C, Corporeau C, Quillien V, Favrel P, Huvet A (2009) In vivo RNA interference in oyster—vasa silencing inhibits germ cell development. FEBS J 276:2566–2573

Feng D, Li Q, Yu H, Zhao X, Kong L (2015) Comparative transcriptome analysis of the Pacific oyster *Crassostrea gigas* characterized by shell colors: identification of genetic bases potentially involved in pigmentation. PLoS One 10:e0145257

Feng D, Li Q, Yu H, Kong L, Du S (2017) Identification of conserved proteins from diverse shell matrix proteome in *Crassostrea gigas*: characterization of genetic bases regulating shell formation. Sci Rep 7:45754

Feng D, Li Q, Yu H, Kong L, Du S (2018) Transcriptional profiling of long non-coding RNAs in mantle of *Crassostrea gigas* and their association with shell pigmentation. Sci Rep 8:1436

Fire A, Xu S, Montgomery MK, Kostas SA, Driver SE, Mello CC (1998) Potent and specific genetic interference by double-stranded RNA in *Caenorhabditis elegans*. Nature 391:806–811

Ge J, Li Q, Yu H, Kong L (2014) Identification and mapping of a SCAR marker linked to a locus involved in shell pigmentation of the Pacific oyster (*Crassostrea gigas*). Aquaculture 434:249–253

Ge J, Li Q, Yu H, Kong L (2015) Identification of single-locus PCR-based markers linked to shell background color in the Pacific oyster (*Crassostrea gigas*). Mar Biotechnol 17:655–662

Gesualdo I, Aniello F, Branno M, Palumbo A (1997) Molecular cloning of a peroxidase mRNA specifically expressed in the ink gland of *Sepia officinalis*. Biochim Biophys Acta 1353:111–117

Hedgecock D, Shin G, Gracey AY, Van Den Berg D, Samanta MP (2015) Second-generation linkage maps for the Pacific oyster *Crassostrea gigas* reveal errors in assembly of genome scaffolds. G3 (Bethesda) 5:2007–2019

Hunter R (1975) Scales for the measurements of color difference. In: Hunter RS (ed) The measurements of appearance. Wiley, New York, pp 133–140

Huvet A, Béguel J-P, Cavaleiro NP et al (2015) Disruption of amylase genes by RNA interference affects reproduction in the Pacific oyster *Crassostrea gigas*. J Exp Biol 218:1740–1747

Ipsaro JJ, Joshua-Tor L (2015) From guide to target: molecular insights into eukaryotic RNA-interference machinery. Nat Struct Mol Biol 22:20–28

Jabbour-Zahab R, Chagot D, Blanc F, Grizel H (1992) Mantle histology, histochemistry and ultrastructure of the pearl oyster *Pinctada margaritifera* (L.). Aquat Living Resour 5:287–298

Knoll AH (2003) Biomineralization and evolutionary history. Rev Mineral Geochem 54:329–356

Li L, Li A, Song K, Meng J, Guo X, Li S, Li C, de Wit P, Que H, Wu F, Wang W, Qi H, Xu F, Cong R, Huang B, Li Y, Wang T, Tang X, Liu S, Li B, Shi R, Liu Y, Bu C, Zhang C, He W, Zhao S, Li H, Zhang S, Zhang L, Zhang G (2018) Divergence and plasticity shape adaptive potential of the Pacific oyster. Nat Ecol Evol 2:1751–1760

McDougall C, Degnan BM (2018) The evolution of mollusc shells. Wiley Interdiscip Rev Dev Biol 7:e313

Palumbo A (2003) Melanogenesis in the ink gland of *Sepia officinalis*. Pigment Cell Res 16:517–522

Papadakis SE (2000) A versatile and inexpensive technique for measuring colour of foods. Food Technol 54:48–51

Payton L, Perrigault M, Bourdineaud J-P, Marcel A, Massabuau J-C, Tran D (2017) Trojan horse strategy for non-invasive interference of clock gene in the oyster *Crassostrea gigas*. Mar Biotechnol 19: 361–371

Pedreschi F, Leon J, Mery D, Moyano P (2006) Development of a computer vision system to measure the color of potato chips. Food Res Int 39:1092–1098

Renault T, Faury N, Barbosa-Solomieu V, Moreau K (2011) Suppression substractive hybridisation (SSH) and real time PCR reveal differential gene expression in the Pacific cupped oyster, *Crassostrea gigas*, challenged with Ostreid herpesvirus 1. Dev Comp Immunol 35: 725–735

Rivera AS, Hammel JU, Haen KM, Danka ES, Cieniewicz B, Winters IP, Posfai D, Wörheide G, Lavrov DV, Knight SW, Hill MS, Hill AL, Nickel M (2011) RNA interference in marine and freshwater sponges: actin knockdown in *Tethya wilhelma* and *Ephydatia muelleriby* ingested dsRNA expressing bacteria. BMC Biotechnol 11:67

Sarathi M, Simon MC, Venkatesan C, Hameed AS (2008) Oral administration of bacterially expressed VP28dsRNA to protect Penaeus monodon from white spot syndrome virus. Mar Biotechnol 10: 242–249

Schmittgen TD, Livak KJ (2008) Analyzing real-time PCR data by the comparative C(T) method. Nat Protoc 3:1101–1108

Schumpert CA, Dudycha JL, Patel RC (2015) Development of an efficient RNA interference method by feeding for the microcrustacean *Daphnia*. BMC Biotechnol 15:91

Slominski A, Tobin DJ, Shibahara S, Wortsman J (2004) Melanin pigmentation in mammalian skin and its hormonal regulation. Physiol Rev 84:1155–1228

Song J, Li Q, Yu Y, Wan S, Han L, Du S (2018) Mapping genetic loci for quantitative traits of golden shell color, mineral element contents, and growth-related traits in Pacific oyster (*Crassostrea gigas*). Mar Biotechnol 20:1–10

Takeo I, Sakai S (1961) Study of breeding of Japanese oyster, *Crassostrea gigas*. Tohoku J Agric Res 12:125–171

Teng W, Cong R, Que H, Zhang G (2018) De novo transcriptome sequencing reveals candidate genes involved in orange shell coloration of bay scallop *Argopecten irradians*. Chin J Oceanol Limnol 36:1408–1416

Tian H, Peng H, Yao Q, Chen H, Xie Q, Tang B, Zhang W (2009) Developmental control of a lepidopteran pest *Spodoptera exigua* by ingestion of bacteria expressing dsRNA of a non-midgut gene. PLoS One 4:e6225

Timmermans A (1998) Computer vision system for on-line sorting of pot plants based on learning techniques. Acta Hortic 421:91–98

Timmons L, Court DL, Fire A (2001) Ingestion of bacterially expressed dsRNAs can produce specific and potent genetic interference in *Caenorhabditis elegans*. Gene 263:103–112

Vavricka CJ, Han Q, Mehere P, Ding H, Christensen BM, Li J (2014) Tyrosine metabolic enzymes from insects and mammals: a comparative perspective. Insect Sci 21:13–19

Wang J, Li Q, Zhong X, Song J, Kong L, Yu H (2018) An integrated genetic map based on EST-SNPs and QTL analysis of shell color traits in Pacific oyster *Crassostrea gigas*. Aquaculture 492:226–236

Williams ST (2017) Molluscan shell colour. Biol Rev 92:1039–1058

Yam KL, Papadakis SE (2004) A simple digital imaging method for measuring and analyzing color of food surfaces. J Food Eng 61: 137–142

Yu H, Zhao X, Li Q (2016) Genome-wide identification and characterization of long intergenic noncoding RNAs and their potential association with larval development in the Pacific oyster. Sci Rep 6: 20796

Zhang G, Fang X, Guo X, Li L, Luo R, Xu F, Yang P, Zhang L, Wang X, Qi H, Xiong Z, Que H, Xie Y, Holland PWH, Paps J, Zhu Y, Wu F, Chen Y, Wang J, Peng C, Meng J, Yang L, Liu J, Wen B, Zhang N, Huang Z, Zhu Q, Feng Y, Mount A, Hedgecock D, Xu Z, Liu Y, Domazet-Lošo T, du Y, Sun X, Zhang S, Liu B, Cheng P, Jiang X, Li J, Fan D, Wang W, Fu W, Wang T, Wang B, Zhang J, Peng Z, Li Y, Li N, Wang J, Chen M, He Y, Tan F, Song X, Zheng Q, Huang R, Yang H, du X, Chen L, Yang M, Gaffney PM, Wang S, Luo L, She Z, Ming Y, Huang W, Zhang S, Huang B, Zhang Y, Qu T, Ni P, Miao G, Wang J, Wang Q, Steinberg CEW, Wang H, Li N, Qian L, Zhang G, Li Y, Yang H, Liu X, Wang J, Yin Y, Wang J (2012) The oyster genome reveals stress adaptation and complexity of shell formation. Nature 490:49–54